

PCCP

Accepted Manuscript



This is an *Accepted Manuscript*, which has been through the Royal Society of Chemistry peer review process and has been accepted for publication.

Accepted Manuscripts are published online shortly after acceptance, before technical editing, formatting and proof reading. Using this free service, authors can make their results available to the community, in citable form, before we publish the edited article. We will replace this *Accepted Manuscript* with the edited and formatted *Advance Article* as soon as it is available.

You can find more information about *Accepted Manuscripts* in the [Information for Authors](#).

Please note that technical editing may introduce minor changes to the text and/or graphics, which may alter content. The journal's standard [Terms & Conditions](#) and the [Ethical guidelines](#) still apply. In no event shall the Royal Society of Chemistry be held responsible for any errors or omissions in this *Accepted Manuscript* or any consequences arising from the use of any information it contains.

Cite this: DOI: 10.1039/x0xx00000x
An IR modulator based on the self-assembly of gold nanoparticles on germanium

000X

Harekrishna Ghosh,^a Ahmed Bouhekka,^{b,c} and Thomas Bürgi*^a

By using a polyelectrolyte layer gold nanoparticles have been assembled onto a Ge internal reflection element. Upon illumination with visible and near infrared light a strong infrared absorption has been observed, which can be traced to intervalence band transitions in Ge. This reveals the existence of holes in the Ge near its valence band edge. The switching between light and dark states is faster than 160 μ s and the device acts as an infrared modulator. The effect develops with a peculiar kinetics, which may indicate the development of an interfacial layer between germanium and gold that allows efficient electron transfer upon illumination.

Received 00th January 2012,
Accepted 00th January 2012

DOI: 10.1039/x0xx00000x

www.rsc.org/

Introduction

Semiconductors are very important because of their wide applications.¹ They are a special class of materials with properties in between conductors and insulators.² The oldest well studied semiconductors are silicon and germanium.³ Silicon has enabled the success of the semiconductor electronics industry. More recently germanium is in the focus again because of its high charge-carrier mobility. Therefore germanium-based transistors are characterized by low energy consumption and high operating speed.⁴ Germanium is also very popular as internal reflection element in infrared spectroscopy.⁵ A lot of research is carried out, in the last years, in order to improve the properties of these materials.⁶ Shining light with an energy equal or bigger than the band gap of a semiconductor leads to the creation of electron-hole pairs,⁷ which is at the origin of numerous applications, ranging from solar energy conversion⁸ over photocatalytic processes⁹ to sensing.¹⁰ Apart from these more traditional applications semiconductors find use in diverse modern applications. They are used for example in epidermal electronic systems that allow electrophysiological measurements,¹¹ which could be used as human/machine interfaces and in integrated devices for genome sequencing.¹²

More recently metal nanoparticles have been used to enhance the properties of semiconductors.¹³⁻¹⁴ In the vicinity of plasmonic metal nanoparticles the electric field is enhanced, which can be used for example in photocatalysis. Indeed, the incorporation of silver nanoparticles can boost photocatalytic activity of TiO₂ significantly, due to the enhanced local electric field.¹⁵ Also, electron transfer between metal nanoparticles and semiconductors is an important issue.¹⁴

Semiconductor – metal composites have properties that strongly depend on the contact between the two materials (formation of space charge regions) and shining light at such

materials can cause a variety of different processes. For Ge – metal interfaces a strong Fermi-level pinning near the valence band edge has been found, which is almost independent of the metal.¹⁶ Furthermore, the insertion of an ultrathin insulating layer between germanium and gold leads to a remarkable shift of the Schottky barrier height.¹⁷ Interface states seem to play an important role in these systems. An interesting option is to use molecules and polymers to modulate this interface because the characteristics of the Ge-Au interface changes significantly by varying the thickness of the insulating layer on the length scale of one nanometer or less.¹⁷

An interesting possibility for applications of semiconductors emerges from the ability to change (modulate) the semiconductor material properties by an external stimulus, which is exploited in the present work. Concretely, the transmittance of germanium in the infrared can be modulated by exciting the semiconductor across its band gap.¹⁸ Such a device acts as a modulator that may find application in infrared imaging techniques. Compared to mechanical chopping, the use of light enables a fast response over large areas apertures without mechanically moving parts.

Here we study the effect of gold nanoparticles assembled on a Ge semiconductor internal reflection element upon visible and near IR light exposure. When the element is illuminated, a drastic absorption of the IR light is observed, which can be traced to holes at the top of the valence band of Ge. The effect develops with a peculiar kinetics, which may be related to the development of a suitable interfacial layer between Ge and the gold nanoparticles. The switching between light and dark phases is very fast and the device acts as an infrared modulator.

Experimental methods

Gold nanoparticles (GNPs), about 20 nm in diameter, were used for our work. GNPs were prepared according to the well-known Turkevich method,¹⁹⁻²¹ and then adsorbed on

functionalized Ge internal reflection elements (IREs; 50 mm × 20 mm × 1 mm, Komlas) which were used for ATR-IR experiments. The IREs were first polished with a 0.25- μm -grain size diamond paste (Buehler, Metadi II) and afterward rinsed copiously with Milli-Q water, before the surface was plasma cleaned under a flow of air for 2 min (Harrick Plasma Cleaner PDC-002). Then the plasma cleaned Ge ATR crystal was functionalized by adsorption of the positively charged polyelectrolyte poly (allyl amine hydrochloride) (PAH). That functionalized Ge surface was used for GNPs adsorption and for further studies. The morphology of the modified Ge surface was characterized by Scanning electron microscopy (SEM, JEOL JSM-7600F¹⁹).

ATR-IR spectra were measured with a Bruker VERTEX 80v Fourier transform infrared (FT-IR) spectrometer with a liquid nitrogen-cooled narrow-band mercury cadmium telluride (MCT) detector. Spectra were recorded at a resolution of 4 cm^{-1} . For in situ ATR-IR experiments a dedicated flow-through cell was used made from a Teflon piece and a fused silica plate (64 mm × 30 mm × 5 mm) with holes for inlet and outlet (39 mm apart), and a Viton seal (1 mm). The volume of the used flow-through cell is 0.129 mL with a gap of 270 μm .²² The cell was mounted on an attachment for ATR measurements within the sample compartment of the FTIR spectrometer. The solutions were passed through the cell and over the Ge crystal at a flow rate of 0.5 ml/min by means of a peristaltic pump (Ismatec, Reglo 100) located in front of the cell. All experiments were performed at room temperature and the spectrometer was evacuated to avoid contributions from gas-phase water and CO_2 .

The illumination of the sample with visible light was carried out using a 300 W Xe arc lamp. The light was guided to the surface using mirrors. To remove any infrared radiation, the light was passed through a 5 cm water filter. A Schott UG 11 (50 mm × 50 mm × 1 mm) broadband filter was used to remove UV light. The irradiance (power per area) of the lamp at the sample was 95 mW/cm^2 as measured by a power meter (818T-10, Newport).

The step-scan technique was used to study the temporal evolution of the system upon illumination. For this the interferometer mirror consecutively steps to the separate points of the interferogram, where the experiment is restarted. To chop the light a chopper was used (Thorlabs MC2F7 blade), which was operated at 400 Hz. The light of the Xe lamp was focused by a 75 mm lens onto the chopper wheel. To reduce the spot size further, a 100 μm slit was placed right in front of the chopper wheel. The data acquisition of the step-scan spectrometer (Bruker VERTEX 80v) was triggered by the chopper. A time resolution of 6 μs was used and per interferometer position, and measurements were done for 72 ms by averaging ten times (ten repetitions). After each change of mirror position a delay of 40 ms was used for stabilization. A resolution of 16 cm^{-1} was applied for the measurements.

Results and discussion

In order to adsorb gold nanoparticles onto the Ge internal reflection element the latter was first polished and then cleaned in an air plasma at reduced pressure. This removes organics and is also thought to lead to a thin oxide layer. In water at neutral pH this surface is negatively charged and in order to adsorb the gold nanoparticles a positively charged polyelectrolyte (PAH) was first adsorbed in situ on the Ge internal reflection element by flowing a PAH solution (1 mg/mL of PAH in 0.1 M NaCl in water) over the sample.²³⁻²⁴ Adsorption is evidenced by *in situ*

ATR measurements (Figure S6, supporting information). Over that modified surface a solution of gold nanoparticles was flown. Adsorption of the gold nanoparticles can be evidenced by the appearance of positive bands associated with water in the ATR spectrum. (Figure S1, supporting information). The appearance of these bands was recently shown to be due to an enhanced infrared absorption from the adsorbed gold nanoparticles.²⁴ We also see signals of citrates (Figure S1), but part of this signal stems from adsorption of free citrate on the PAH and is therefore not a good measure for gold nanoparticle adsorption. Adsorption of gold nanoparticles was also evidenced by scanning electron microscopy (SEM). Figure 1 shows the SEM images of GNPs adsorbed on a functionalised Ge ATR crystal surface. The spherical GNP of around 20 nm in diameter are well dispersed. This is due to the mutual repulsion between adsorbed nanoparticles as a consequence of Coulomb interaction. The particle density on the surface is 650 particles/ μm^2 , which corresponds to a coverage of about 20%. The scratches on the Ge surface originating from the polishing process are clearly visible. Note that gold nanoparticle adsorption was not observed when the surface was charged negative by adsorption of a negative polyelectrolyte on top of PAH.

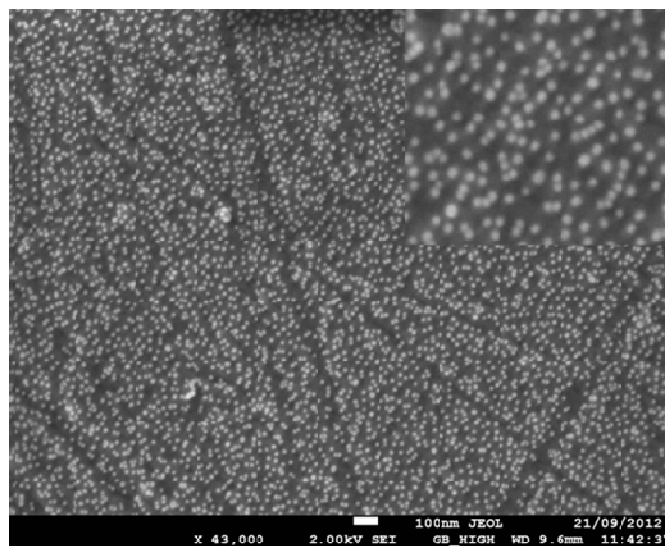


Figure 1. SEM image of GNPs on a functionalized Ge surface. The Ge ATR crystal was plasma cleaned before PAH functionalization. After 40 minutes of GNP adsorption the crystal surface was washed with copious amounts of neat water. The scale bar corresponds to 100 nm. The inset (top right) shows a magnification of the image.

After adsorption of the gold nanoparticles, and a washing step with neat water for about 90 min a background was taken in the dark, and the IR spectrum was measured during the irradiation of the Ge internal reflection element with a Xe lamp. Irradiation had a drastic effect, as can be seen in Figure 2. Three broad bands can be observed at about 3000 cm^{-1} , 2130 cm^{-1} and 920 cm^{-1} . Note that at the latter wavenumber the sensitivity of the MCT detector drops and therefore the maximum of the latter band could be at lower wavenumbers. The IR spectrum emerging upon illumination with visible light corresponds to the one observed for p-type germanium,¹⁸ which indicates that

upon illumination the top of the valence band is occupied by holes. The top of the valence band of Ge is characterized by three sub-bands. Two bands are formed from the $p_{3/2}$ level of the Ge atoms and are associated with holes characterized by two different effective masses, heavy and light. A third band derives from the $p_{1/2}$ level and is split off the other two bands by spin-orbit interaction.²⁵ The three bands observed in the infrared spectrum (Figure 2) arise from the transitions between these bands (intervalence band transitions) and are assigned as heavy hole – spin orbit (3000 cm^{-1}), light hole – spin orbit (2130 cm^{-1}) and heavy hole – light hole (920 cm^{-1}) transitions.¹⁸ The absorption is a direct measure of the density of holes.²⁶ The lowest energy band centred around 920 cm^{-1} shows an absorbance of almost 20% under the applied conditions (Figure 2). The absorption cross section of electrons is more than one order of magnitude smaller at 920 cm^{-1} than the one for holes, and therefore the spectrum is largely dominated by hole absorption.²⁷ Note that both the gold nanoparticles and the Ge absorb light. However, a monolayer of gold nanoparticles shows an extinction of about 0.05 only.²³ Therefore, most of the light is absorbed by the Ge.

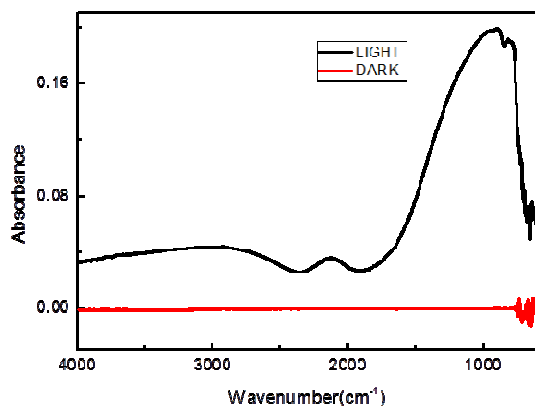


Figure 2. ATR-IR spectra of a Ge internal reflection element functionalized by PAH polyelectrolyte and gold nanoparticles. The red curve corresponds to the background recorded in the dark, whereas the black curve was recorded during illumination by a Xe lamp.

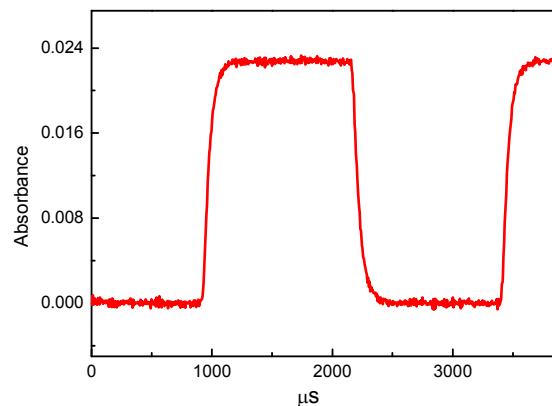


Figure 3: Absorbance at 1000 cm^{-1} as a function of time measured in a step-scan experiment. The frequency was set to 400 Hz using a chopper (Thorlabs MC2F7 blade) and a time-resolution of $6\text{ }\mu\text{s}$ was used.

The observed effect is instantaneous to within the time-resolution of the instrument. The switching between the “dark” and “light” state takes place within less than the time needed for the instrument to record a full interferogram (about 50 ms , depending on the parameters). We therefore performed some step-scan experiments using a chopper. Due to the finite size of the focus of the lamp at the chopper blade and the chopper speed a maximum time-resolution of about $150\text{ }\mu\text{s}$ could be achieved. The process is at least as fast as that as can be seen from Figure 3.

The role of the gold nanoparticles for the phenomena was furthermore investigated. The experiment was therefore repeated in an identical fashion except for the adsorption of the gold nanoparticles, which was omitted. The experiment was furthermore repeated for a clean Ge internal reflection element. Figure 4 shows the results of these experiments, in comparison with an experiment in the presence of gold nanoparticles. Without the adsorbed gold nanoparticles the band centred at 920 cm^{-1} is also observed, although less intense by two orders of magnitude. As concerns the two other bands, they can also be deciphered, although less clearly due to the small signals and other spectral contributions from water. The observation of the intervalence band transitions upon illumination of Ge by visible light is not surprising, because holes are created in the valence band due to excitation of electrons across the band gap. The astonishing point is the observation that the signal of holes in Ge is increased by two orders of magnitude, by the adsorption of gold nanoparticles on its surface. This could be either due to the increased concentration of holes or an increased cross section of the holes due to enhancement by the gold nanoparticles. Indeed, we have observed enhancement of water and polyelectrolyte signals by gold nanoparticles adsorbed on Ge.²⁴ However, these enhancements were moderate, far below the two orders of magnitude observed here. More importantly, the enhancement is strictly correlated with the concentration adsorbed gold nanoparticles, which is not the case here (see below). We therefore think that the increased concentration of holes is the dominant contribution to signal.

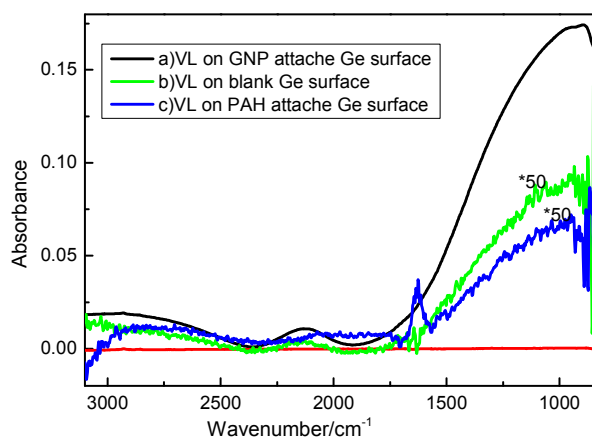


Figure 4. Effect of visible light on blank Ge, Ge functionalized by PAH and by PAH and gold nanoparticles. For each spectrum a background was taken in the dark. The spectra without the gold nanoparticles were scaled by a factor of 50.

We furthermore observed that once the effect was established, after preparing the gold nanoparticle layer on the Ge internal reflection element in situ by the wet chemical process, the element could be removed from the cell and dried without loss of the infrared absorption upon visible light excitation. In the dry state the gold nanoparticles were partly removed mechanically by applying a scotch tape. Removal of particles was evident from the color of the tape and lead to a decrease of the absorption bands in the infrared spectrum upon illumination with the Xe lamp, as can be seen in Figure 5. Experiments were furthermore done by adsorbing less gold nanoparticles in the first place, by reducing the time of adsorption. The coverage was estimated from the enhanced water signal. By adsorbing 15% (70%) of a full coverage the hole absorption in Ge saturated at 3.7 % (15%) instead of 20% for a full coverage. This observation corroborates the importance of the gold nanoparticles in the process.

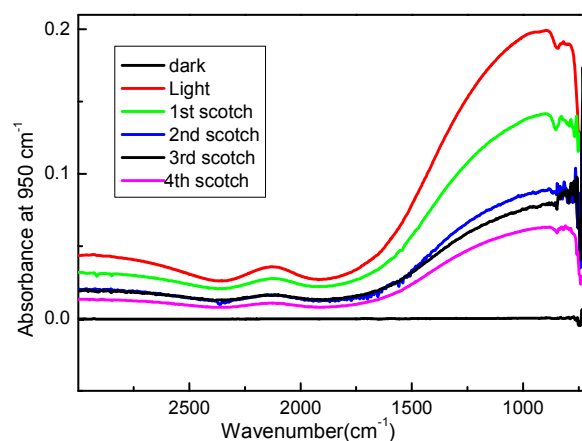


Figure 5. ATR-IR spectra of the dry sample (Ge, PAH polyelectrolyte, gold nanoparticles) upon illumination with a Xe lamp. The background was taken before illumination in the dark. Shown are the spectra of the as prepared sample and after different steps of removal of gold nanoparticles by scotch tape.

The experiments described above indicate the importance of the gold nanoparticles, for the observed drastically increased signal of holes in Ge upon illumination. A similar effect was observed when silver nanoparticles were used instead of gold (Figure S2, supporting information), however, in this case the absorbance due to the holes in Ge was slightly weaker, amounting to 15% at 950 cm^{-1} instead of 18-20% in the case of gold nanoparticles. It was furthermore found that the presence of the particles is not sufficient for the observation of the effect. We observed that the strong IR absorption due to the holes in the valence band of Ge upon illumination develops with time after adsorption of the gold nanoparticles and rinsing with neat water. Figure 6 shows both the kinetics of the nanoparticle adsorption and the development of the IR absorbance upon illumination. Both were measured during the same experiment. For the kinetics of the gold nanoparticle adsorption, the absorbance of the water band at 1640 cm^{-1} was plotted against time. We have shown before that the gold nanoparticles lead to an enhanced IR absorption of the water phase surrounding the nanoparticles.²⁴ Adsorption is fast and almost complete after five minutes. In contrast, the increase of the hole concentration at the valence band edge of Ge upon illumination is observed much later, with a completely different kinetics as compared to nanoparticle adsorption. The effect starts to increase about 20 minutes after complete adsorption of gold nanoparticles. Then the increase becomes more pronounced till reaching saturation after about 90 min. For this experiment the sample was illuminated during the measurement of the IR spectra, but was in the dark in between the measurements. However, the experiment was repeated with the sample completely in the dark for 100 min. After that the strong IR absorption was observed upon illumination (Figure S3, supporting information). This shows that other factors than light are responsible for peculiar kinetics shown in Figure 6.

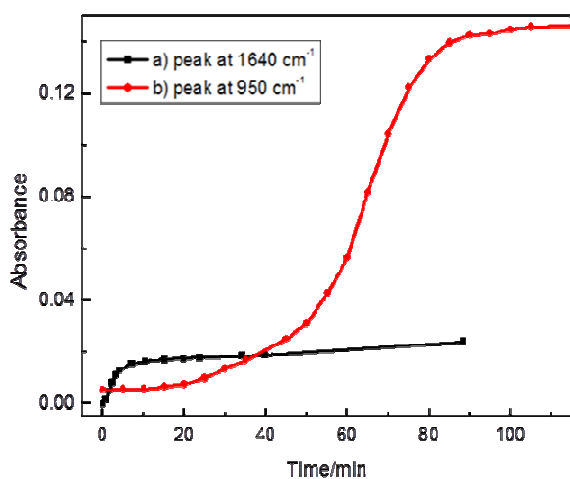


Figure 6. Kinetics of gold nanoparticle adsorption and IR absorption upon illumination due to valence band holes in Ge measured by ATR-IR spectroscopy. The kinetics of gold nanoparticle adsorption is represented by the peak absorbance of the band at 1640 cm^{-1} due to water. These measurements were performed in the dark. The development of the IR absorption upon illumination was followed by plotting the absorbance at 950 cm^{-1} associated with hole in Ge. Time $t=0$ refers to the start of gold nanoparticle adsorption.

The absorbance in the infrared is proportional to the irradiance in the visible / NIR as was verified by using gray filters (Figure S4, supporting information). Figure 7 shows the absorbance at 950 cm^{-1} as a function of the transmittance of the used gray filters, which is a measure of the power incident on the surface of the gold nanoparticle modified Ge internal reflection element.

The behavior described above is the one of a modulator of the IR light driven by visible / NIR light. In the present study the irradiance of the Xe lamp incident on the sample was measured to be 95 mW/cm^2 , which modulated the absorbance at 1000 cm^{-1} ($10\text{ }\mu\text{m}$) by about 20%. More intense light sources would lead to higher modulation amplitudes. The most interesting aspect of the work is however the drastic increase of the concentration of valence band holes upon illumination when the Ge surface is treated by gold nanoparticles. The particles could act in different ways. First of all the particles bear a plasmon resonance, and the enhanced electric field in the vicinity of the gold particles upon illumination could lead to enhanced absorption of light by the Ge semiconductor. The direct involvement of the plasmon of the gold nanoparticles in the process would be reflected in a characteristic wavelength dependency. In particular the most prominent IR absorption should be observed when exciting the plasmon of the gold nanoparticles, which is around 520 nm in solution and around 580 nm when adsorbed on the Ge, due to its high refractive index (see reflectance spectra, Figure S8, supporting information). We therefore studied the wavelength-dependence using band pass filters. Such a wavelength-dependence is not observed (Figure S5, supporting information) and therefore the direct involvement of the plasmon in this process is not indicated. A more likely process is transfer of electrons from

the Ge to the gold nanoparticles, after excitation of the Ge semiconductor and the creation of an electron – hole pair. In such a way the hole is left behind in the Ge and recombination is slowed down. Ge has an electron affinity of 4 eV and a band gap of 0.66 eV ,²⁸⁻²⁹ and gold has a work function of 5.1 eV . Therefore excited electrons in the conduction band of Ge should have enough energy to transfer to the gold nanoparticles. The same arguments hold for silver nanoparticles, however, in this case the work function is smaller (4.7 eV). The reduced driving force in that case might explain the weaker IR absorption in the presence of silver nanoparticles (15%) compared to gold (20%). The mechanism discussed above implies an electron transfer through the gap between the Ge surface and the gold (or silver) nanoparticles. The nature of this gap is quite complex consisting possibly of a thin oxide layer on the Ge and the PAH polyelectrolyte. The peculiar kinetics shown in Figure 6 with a characteristic time needed to fully establish the effect might be due to the nature of this Ge – gold nanoparticle gap, which does not allow electron transfer right after the adsorption of the gold nanoparticles. This would indicate that the gap undergoes some transformation within about 90 minutes after the adsorption of the gold nanoparticles. In this context we should mention that the observations are reproducible. More than twenty experiments were performed using different Ge internal reflection elements and the effect was always observed. In these experiments the absorbance varied between 16% and 20%. We furthermore tried to enhance the effect by adsorbing multiple GNP layers (with PAH layers in between), but the effect could not be enhanced significantly. It is interesting to compare the modulation depth obtained with our samples to the one reported before for Ge,¹⁸ although both the materials and measurement geometries are different. To obtain large modulation depths with Ge alone one has to achieve long carrier lifetimes, which usually requires high purity Ge and very careful treatment of the sample surface. The latter is important because carriers are generated within about $1\text{ }\mu\text{m}$ of the surface and therefore surface recombination needs to be avoided, which requires a careful etching of the surface. Using 9.6 Wcm^{-2} at 980 nm an absorbance of close to 1 could be achieved in transmission mode using high purity Ge and careful surface treatment.¹⁸ In our case we obtained an absorbance of 0.2 in ATR mode with 96 mWcm^{-2} , using optical grade Ge without etching procedures. Considering that in the ATR experiment we have about 16 reflections and that for each reflection the beam is transmitting the Ge surface region twice (before and after reflection) we expect a change by a factor of $16 \times 2 = 32$ due to the different geometry of the two measurements. The two measurements were also done at different irradiance, 9.6 Wcm^{-2} compared to 96 mWcm^{-2} , which represents a factor of 100. Taking both aspects into account we can expect a factor of $32/100 = 0.32$, which is actually quite close to the measured ratio of the absorbance values for the two measurements. Despite the comparable efficiency of the two samples there is a clear difference in the switching speed. Whereas it takes less than $200\text{ }\mu\text{s}$ to fully switch our sample with the nanoparticles, the carefully surface treated high purity Ge takes about 4 ms to fully relax.

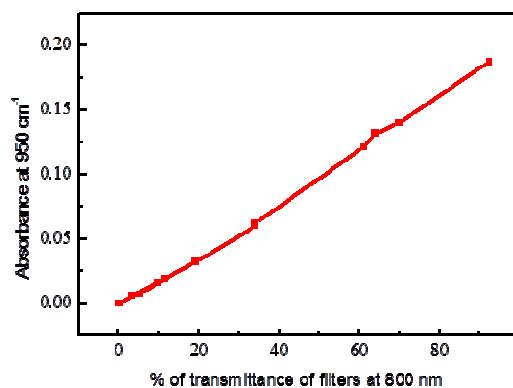


Figure 7. Transmittance of filters vs peak-absorbance at 950 cm^{-1} during illumination.

Conclusions

Gold nanoparticles were assembled on Ge internal reflection elements, by using positively charged polyelectrolyte as intermediate layer. Upon illumination with visible and near IR light strong infrared absorption bands can be observed, that reflect the presence of holes near the valence band edge in germanium. Without the nanoparticles the same IR bands can be observed when illuminating the internal reflection element, due to excitation of the semiconductor across the band gap. However, in the presence of the gold nanoparticles the effect is two orders of magnitude larger. The observed effect is well reproducible and robust. The internal reflection element acts as an IR modulator triggered by visible or near IR light. The modulation depth is comparable to the one reported for high purity Ge that was carefully surface treated. However, much higher modulation rates can be achieved with the nanoparticles because of a much larger relaxation rate. It is believed that electron transfer from the germanium to the gold nanoparticles plays an important role in this process. A peculiar kinetics is observed for the development of the effect once the nanoparticles are adsorbed, with an initially very weak modulation depth that develops with time. The complex interlayer composed of water, citrate and polyelectrolyte possibly plays a crucial role because it can affect the electron transfer between germanium and the gold nanoparticles, and it can affect the pinning of the metal Fermi level through the modulation of interfacial states.

Acknowledgements

This work was supported by the University of Geneva and the Swiss National Science Foundation.

Notes and references

^a Département de Chimie Physique, Université de Genève, 30 Quai Ernest-Ansermet, 1211 Genève 4, Switzerland

^b Laboratoire de Physique des Couches Minces et Matériaux pour l'Electronique, Université d'Oran Es-Senia, 31100 Oran, Algeria

^c Département de Physique, Faculté des Sciences, Université Hassiba Ben Bouali, 02000 Ouled Fares-Chlef, Algeria

Electronic Supplementary Information (ESI) available: Additional ATR spectra, transmittance of gray filters, wavelength dependence of IR absorbance. See DOI: 10.1039/b000000x/

1 W. Shockley, *Electrons and Holes in Semiconductors*, John Wiley, Princeton, 1950.

2 J. Singh, *Electronic and optoelectronic properties of semiconductor structures*, Cambridge university press, New York, 2003.

3 K. Seeger, *Semiconductor Physics*, Springer, Berlin, 1991.

4 R. Pillarisetty, *Nature*, 2011, **479**, 324-328.

5 I. Dolamic, C. Gautier, J. Boudon, N. Shalkevich and T. Bürgi, *J. Phys. Chem. C*, 2008, **112**, 5816-5824.

6 C. Droz, M. Goerlitzer, N. Wyrsh and A. Shah, *J. Non-Cryst. Solids*, 2000, **266–269, Part 1**, 319-324.

7 J. Faist, *Optical Properties of Semiconductors*, Eidgenössische Technische Hochschule Zürich, Zürich, May 2008.

8 A. Shah, P. Torres, R. Tschamer, N. Wyrsh and H. Keppner, *Science*, 1999, **285**, 692-698.

9 S. Y. Reece, J. A. Hamel, K. Sung, T. D. Jarvi, A. J. Esswein, J. J. H. Pijpers and D. G. Nocera, *Science*, 2011, **334**, 645-648.

10 W. Jaimes Salcedo, F. J. Ramirez Fernandez and J. C. Rubim, *Spectrochim. Acta Mol.*, 2004, **60**, 1065-1070.

11 D.-H. Kim, N. Lu, R. Ma, Y.-S. Kim, R.-H. Kim, S. Wang, J. Wu, S. M. Won, H. Tao, A. Islam, K. J. Yu, T.-i. Kim, R. Chowdhury, M. Ying, L. Xu, M. Li, H.-J. Chung, H. Keum, M. McCormick, P. Liu, Y.-W. Zhang, F. G. Omenetto, Y. Huang, T. Coleman and J. A. Rogers, *Science*, 2011, **333**, 838-843.

12 J. M. Rothberg, W. Hinz, T. M. Rearick, J. Schultz, W. Mileski, M. Davey, J. H. Leamon, K. Johnson, M. J. Milgrew, M. Edwards, J. Hoon, J. F. Simons, D. Marran, J. W. Myers, J. F. Davidson, A. Branting, J. R. Nobile, B. P. Puc, D. Light, T. A. Clark, M. Huber, J. T. Branciforte, I. B. Stoner, S. E. Cawley, M. Lyons, Y. Fu, N. Homer, M. Sedova, X. Miao, B. Reed, J. Sabina, E. Feierstein, M. Schorn, M. Alanjary, E. Dimalanta, D. Dressman, R. Kasinskas, T. Sokolsky, J. A. Fidanza, E. Namsaraev, K. J. McKernan, A. Williams, G. T. Roth and J. Bustillo, *Nature*, 2011, **475**, 348-352.

13 P. V. Kamat, *J. Phys. Chem. B*, 2002, **106**, 7729-7744.

14 X. Zhang, Y. L. Chen, R.-S. Liu and D. P. Tsai, *Rep. Prog. Phys.*, 2013, **76**, 046401.

15 K. Awazu, M. Fujimaki, C. Rockstuhl, J. Tominaga, H. Murakami, Y. Ohki, N. Yoshida and T. Watanabe, *J. Am. Chem. Soc.*, 2008, **130**, 1676-1680.

16 T. Nishimura, K. Kita and A. Toriumi, *Appl. Phys. Lett.*, 2007, **91**, 123123.

17 T. Nishimura, K. Kita and A. Toriumi, *Appl. Phys. Express*, 2008, **1**, 051406.

18 P. D. Fairley and H. N. Rutt, *J. Phys. D: Appl. Phys.*, 2000, **33**, 2837-2852.

19 J. Turkevich, P. C. Stevenson and J. Hillier, *Discuss. Faraday Soc.*, 1951, **11**, 55-75.

Journal Name

- 20 J. Kimling, M. Maier, B. Okenve, V. Kotaidis, H. Ballot and A. Plech, *J. Phys. Chem. B*, 2006, **110**, 15700-15707.
- 21 G. Frens, *Nature. physical science*, 1973, **241**, 20-22.
- 22 B. Völker, F. Wölzl, T. Bürgi and D. Lingenfeller, *Langmuir*, 2012, **28**, 11354-11363.
- 23 A. Cunningham, S. Mühlig, C. Rockstuhl and T. Bürgi, *J. Phys. Chem. C*, 2011, **115**, 8955-8960.
- 24 H. Ghosh and T. Bürgi, *J. Phys. Chem. C*, 2013, **117**, 26652-26658.
- 25 C. Kittel, Introduction to solid state physics, John Wiley, New York, 1996.
- 26 A. H. Kahn, *Physical Review*, 1955, **97**, 1647-1652.
- 27 C. J. Hutchinson, C. Lewis, J. A. Savage and A. Pitt, *Appl. Opt.*, 1982, **21**, 1490-1495.
- 28 S. M. Sze, Physics of Semiconductor Devices, John Wiley & Sons, 1981.
- 29 S. Wolf and R. Tauber, Silicon Processing for the VLSI Era, Lattice Press, Sunset Beach, California, 1986.